Kütahya Dumlupınar University
Institute of Graduate Studies

Journal of Scientific
Reports-A
E-ISSN: 2687-6167
Number 54, September 2023

RESEARCH ARTICLE

NUMERICAL MODELING OF BACKWARD-FACING STEP FLOW VIA COMPUTATIONAL FLUID DYNAMICS

Ilker GOKTEPELI[1*], Ulas ATMACA[2]

[1*]Konya Technical University, Faculty of Engineering and Natural Sciences, Department of Mechanical Engineering, Konya, igoktepeli@ktun.edu.tr, ORCID: 0000-0002-2886-8018
[2]Konya Technical University, Faculty of Engineering and Natural Sciences, Department of Mechanical Engineering, Konya, suatmaca@ktun.edu.tr, ORCID: 0000-0002-9265-1446

Receive Date: 21.05.2023 *Accepted Date: 18.08.2023*

ABSTRACT

As a fundamental case for problems of fluid mechanics, examination of flow separation and its reattachment is important for engineering applications. Considering the significance of the subject, backward-facing step flow has been modeled via Computational Fluid Dynamics (CFD) based on an experimental study previously done at Re = 5000. Steady simulations have been conducted by k-ε Renormalization Group (RNG) considering the same flow conditions of the reference study. Pressure distributions, streamwise and cross-stream velocity components, velocity magnitude values with streamline patterns and turbulence kinetic energy values have been presented by using contour graphics. Furthermore, the stations for pressure distributions, velocity profiles for streamwise components and turbulence kinetic energy values have been defined for evolution of related data. Lower pressure zone for the wake region of the backward-facing step has been attained due to flow separation. Separation of the upstream boundary layer has been seen and it became a curved one. Moreover, turbulence level of the step wake has been obtained as higher than those of any other points. Transition to core flow has been attained at $y^* = 1.1$ that is above the step height. Flow oscillations have been observed for $x^* \geq 2$ and $y^* \leq 1$ since the fluctuations for these values were effective in the wake region. To sum up, the dimensionless reattachment length has been numerically obtained as 5.92 which is very good agreement with the experimental results at same Reynolds number. The deviation from the reference results is from 0.34 % to 1.33 %.

Keywords: *Backward-facing step, Flow separation, k-ε RNG, Reattachment length, Turbulence*

1. INTRODUCTION

Flow separation and its reattachment is a fundamental phenomenon for fluid mechanics and heat transfer problems. These problems are considered as significant for modern engineering applications. Backward-facing step flow is one of the cases that flow separation and flow reattachment are noteworthy. These flow structures are influenced by geometric design, expansion ratio, flow

JSR A
Journal of Scientific Reports

characteristics as well as thermal conditions [1-2]. This type of flow is frequently observed in the studies related to aerodynamics and hydrodynamics. For this reason, backward-facing step flow is encountered in aeronautical, civil, mechanical and naval engineering disciplines such as airfoils, buildings, heat exchangers, hydrofoils, spoilers [1]. What is more, the present case is related to turbine blades, combustor flame-holder and engine inlets [3]. Furthermore, it is possible to associate this subject to ecological, hydrological and also meteorological issues [4]. Several designs are also used to decrease the velocity of fluid flow [5]. A micro combustor has also been presented as a backward-facing step [6-7]. Based on these usage examples, controlling shear flows is very important for industrial applications [8]. At the upstream of a backward-facing step, there is detached boundary layer. However, recirculation region including one or more vorticities occurred at the downstream due to the backward-facing step. Then, separated flow owing to this step reattaches at a point in the wake region [9].

Over the decades, the present problem has been researched in the experimental, numerical and theoretical studies of open literature. In terms of experimental studies, Jovic and Driver [10] have examined the influence of Reynolds number on skin friction measurements for $5000 \leq Re \leq 37200$. They have used Laser-Oil Flow Interferometry (LOI) method for backward-facing step flow. Kasagi and Matsunaga [11] have used particle tracking velocimeter for three-dimensional backward-facing step flow at Re = 5540. They have compared experimental results with the ones obtained via Direct Numerical Simulation (DNS) from open literature. Scarano et al. [12] have implemented a pattern recognition technique for flow past a backward-facing step. For Re = 5000, Digital Particle Image Velocimetry (DPIV) has been used. Wengle et al. [13] have examined backward-facing step flow by the wind tunnel experiments and compared these results with the numerical ones of DNS at Re = 3000. Kostas et al. [14] have experimentally studied on backward-facing step flow by using Particle Image Velocimetry (PIV) at Re = 4660. Furuichi et al. [15] have measured velocity fields of separated shear layer and flow reattachment zone for a backward-facing step. They have used Laser Doppler Velocimetry (LDV) in terms of two-dimensional case at Re = 5000. It was concluded that large-scale fluctuations could be modeled via a model proposed by the authors. Same method has also been utilized by Nie and Armaly [16]. Three-dimensional backward-facing step flow has been investigated from Re = 100 to Re = 8000. The aim of their study is to capture the boundaries of reverse flow zones. Schram et al. [17] have done PIV experiments for flow over a backward-facing step at Re = 5100. Bouda et al. [18] have used Laser Doppler Anemometry (LDA) for turbulent jet flow past a backward-facing step at Re = 7600. Experimental results have been compared with the numerical ones of RANS simulations. Wu et al. [19] have conducted experiments about backward-facing step flow via PIV at Re = 3450. They have examined the effect of smooth and rough surfaces on flow characteristics. Nadge and Govardhan [20] have experimentally investigated flow structure for the wake region of a backward-facing step via PIV. For different Reynolds numbers, the results have been presented. Yamada and Nakamura [21] have measured heat transfer and flow characteristics in the wake region of a backward-facing step from Re = 2500 to Re = 5200.

When it comes to numerical studies about backward-facing step flow, Le et al. [22] have utilized DNS to examine turbulent flow of a backward-facing step at Re = 5100. Chiang et al. [23] have conducted numerical analyses for backward-facing step flow at $50 \leq Re \leq 2500$. Avancha and Pletcher [24] have numerically studied on the same problem for Re = 5540. In a study including the case of heat transfer,

JSR A
Journal of Scientific Reports

LES turbulence model has been implemented. Dejoan and Leschziner [25] have used LES turbulence model for the same case at Re = 3700. Aider and Danet [26] have performed numerical analyses by using LES model for flow over a backward-facing step at Re = 5100. Barri et al. [27] have numerically studied on flow past a backward-facing step. DNS has been used in their study for Reynolds number of 5600. El Khoury et al. [28] have utilized DNS to consider backward-facing step flow at Re = 5200. Jürgens and Kaltenbach [29] have employed LES turbulence model for backward-facing step flow of Re = 3000. LES turbulence model has also been used by Kanchi et al. [30] for backward-facing step flow for varying Reynolds numbers from 5000 to 28000. Togun et al. [31] have numerically studied on backward-facing step flow for laminar and turbulent flow of heat transfer problem. In their study for turbulent flow, they have used k-ω Shear Stress Transport (SST) turbulence model. Amiri et al. [32] have presented a study with experimental and numerical parts for heat transfer of backward-facing step flow in terms of various Reynolds number values. Xu et al. [33] have established a numerical model for three-dimensional backward-facing step flow. Several Reynolds numbers have been considered for the case including heat transfer.

The aim of the study is to examine the backward-facing step flow that is very important for engineering applications owing to flow separation and its reattachment. It is well known that flow behavior is affected by the change of channel height for flow direction. Therefore, this effect should be considered and investigated by using experimental and numerical techniques. Due to non-availability of experimental facilities, numerical modeling with reliable methods is crucial. At the present Reynolds number for the present case, various turbulence models have been tested. As a result, k-ε Renormalization Group (RNG) turbulence model has been implemented for the numerical study since the numerical results have been validated with respect to the experimental outcomes of the literature.

2. NUMERICAL METHOD

Backward-facing step flow has been numerically investigated at Re = 5000. Turbulence models based on k-ε and k-ω methods have been compared. After the comparison of these models, k-ε RNG turbulence model has been used for numerical simulations conducted in ANSYS-Fluent 21. As a reference study, research presented by Furuichi et al. [15] has been considered and the numerical results have been compared and validated.

2.1. Turbulence Model

Continuity and momentum equations have been solved. In this process, Reynolds-Averaged Navier-Stokes (RANS) equations are utilized. In case of incompressible flow conditions, aforementioned equations have been considered with Eqs. 1-2, respectively [34-35]:

$$\frac{\partial \rho}{\partial t} + \frac{\partial}{\partial x_i}(\rho u_i) = 0 \tag{1}$$

$$\frac{\partial}{\partial t}(\rho u_i) + \frac{\partial}{\partial x_i}(\rho u_i u_j) = -\frac{\partial \rho}{\partial x_i} + \frac{\partial}{\partial x_j}\left[\mu\left(\frac{\partial u_i}{\partial x_j} + \frac{\partial u_j}{\partial x_i} - \frac{2}{3}\delta_{ij}\frac{\partial u_l}{\partial x_l}\right)\right] + \frac{\partial}{\partial x_j}\left(-\rho\overline{x_i' x_j'}\right) \tag{2}$$

JSR A
Journal of Scientific Reports

Turbulent stresses have to be included for the solution process. Turbulence models are the methods providing these terms for the solution. As a k-ε based method, k-ε RNG turbulence model has been used in the present study. The difference between the k-ε RNG model and standard k-ε model is related to analytical derivation for the technique with the constants, the additional terms and the functions in the equations of transport as in Eqs. 3-4 [34].

$$\frac{\partial}{\partial t}(\rho k) + \frac{\partial}{\partial x_i}(\rho k u_i) = \frac{\partial}{\partial x_i}\left[\mu_{eff}\alpha_k \frac{\partial k}{\partial x_j}\right] + G_k - \rho\varepsilon + S_k \tag{3}$$

$$\frac{\partial}{\partial t}(\rho \varepsilon) + \frac{\partial}{\partial x_i}(\rho \varepsilon u_i) = \frac{\partial}{\partial x_i}\left[\mu_{eff}\alpha_k \frac{\partial \varepsilon}{\partial x_j}\right] + C_{1\varepsilon}G_k \frac{\varepsilon}{k} - C_{2\varepsilon}\rho\frac{\varepsilon^2}{k} - R_\varepsilon + S_\varepsilon \tag{4}$$

The RNG turbulence model could be considered as the refinement of its standard method. Moreover, it shows more sensitivity for the estimation of the effects of rapid strain and streamlines curvature compared to the properties of the standard model [34].

2.2. Flow Domain

Flow domain has been defined as three-dimensional with respect to a study experimentally done by Furuichi et al. [15]. Its dimensions are $-12.5 \leq x^* = x/h \leq 12.5$ in streamwise direction and $-6 \leq z^* = z/h \leq 6$ in spanwise direction. What is more, these are $0 \leq y^* = y/h \leq 2$ and $0 \leq y^* = y/h \leq 3$ for the upstream ($-12.5 \leq x^* \leq 0$) and the downstream ($0 \leq x^* \leq 12.5$) regions of the step height in cross-stream direction, respectively. These dimensions are non-dimensional by considering the step height which is h = 0.02 m. Schematic view of the model has been given in Figure 1.

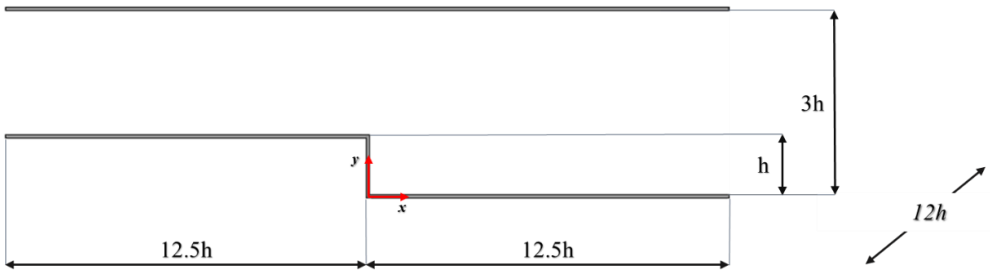

Figure 1. Schematic view of the model.

For the inlet, U_∞ = 0.25 m/s has been defined as uniform velocity at Reynolds number of $Re_h = U_\infty h / \nu$ = 5000 based on a step height. Kinematic viscosity of water is considered. Pressure outlet has been used as boundary condition to provide gauge pressure at the channel exit that is open to atmosphere. No-slip boundary condition has been applied for the channel walls.

Numerical solution is performed via uniform or non-uniform grid elements covering the geometry of the problem [36-37]. Therefore, grid independence study is very crucial for the reliability of the numerical simulations. For the present study, the numbers of grid elements of 4 500 000, 6 000 000 and 8 200 000 have been contrasted via reattachment length ($x_r^* = x_r/h$) presented in the reference

JSR A
Journal of Scientific Reports

study. After the flow separation from the backward-facing step, flow reattaches to the bottom surface of the duct downstream. The reattachment length is measured between the flow separation from the step and the reattachment point. When the value for wall shear stress (τ) is zero at any point, the difference between the origin and this point indicates the reattachment length. By the way, wall shear stress has also been given in non-dimensional form as $\tau^* = \tau / (\rho U_\infty^2)$ where water density and uniform inlet velocity are used. As an example, the downstream results obtained by the k-ε RNG turbulence model have been presented in Figure 2.

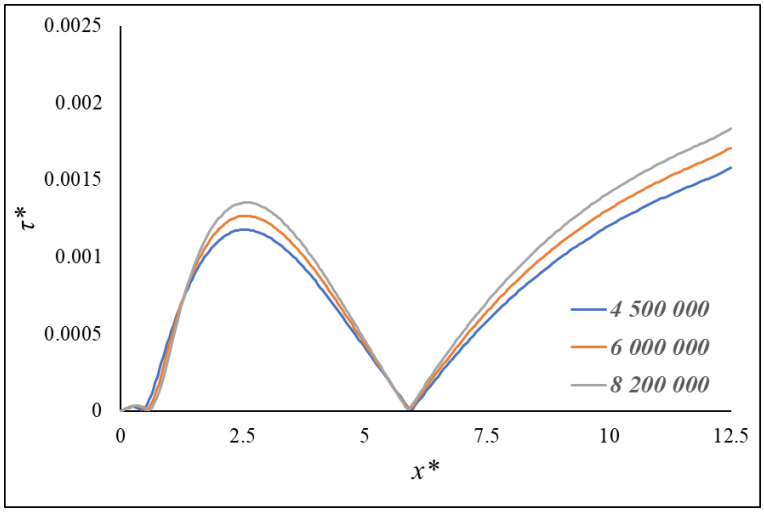

Figure 2. Grid independence test for wall shear stress at y* = z* = 0.

The experimental result for the reattachment length has been obtained as $x_r^* = 6$ by Furuichi et al. [15]. For this reason, this value has been accepted as the reference value for grid independence test. The closest value to the experimental result has been attained as $x_r^* = 5.92$ by using the number of grid elements as 6 000 000 with respect to the results. The grid system has been presented in Figure 3.

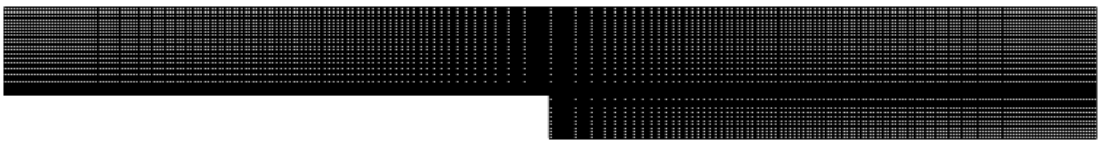

Figure 3. The grid structure on x-y plane.

What is more, the residuals of all equations have been taken as 10^{-6} throughout the steady simulations. Moreover, the turbulence models based on k-ε and k-ω methods have been compared in terms of wall shear stress values. As an example, the results obtained via the number of grid elements as 6 000 000 have been shown. In Figure 4, the comparison chart has been given for Standard k-ε, k-ε RNG, k-ε Realizable, Standard k-ω and k-ω SST turbulence models.

JSR A
Journal of Scientific Reports

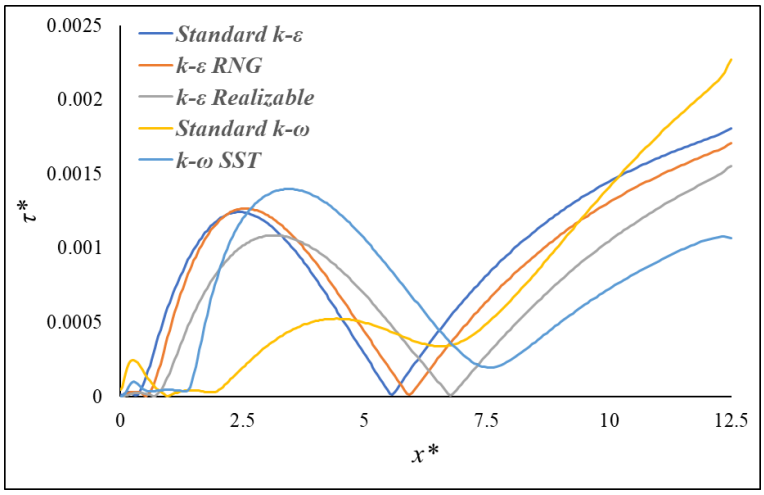

Figure 4. Wall shear stress for various turbulence models at y* = z* = 0.

With respect to these results, the turbulence models based on k-ω are failed to capture the reattachment length when it is compared to the result of the reference study. Relatively, the turbulence models based on k-ε are more successful. Nonetheless, k-ε Realizable turbulence model is the third one among the investigated ones in case of reattachment length. As a result, the closest result to the reference value has been attained by using k-ε RNG turbulence model.

2.3. Validation

Hydrodynamic flow characteristics for a backward-facing step has been investigated via k-ε RNG turbulence model. The aspect ratio is obtained by the division of spanwise length to the step height as AR = 12 while the expansion ratio is given by the ratio of the duct height of downstream to the duct height of upstream as ER = 1.5 as in the reference experimental study. The flow domain has been established by considering the dimensions with those used by Furuichi et al. [15]. Dimensionless values for reattachment length have been given in Table 1.

Table 1. Dimensionless reattachment length values at similar Reynolds numbers.

	Method	Re	AR	ER	x_r^*
Scarano et al. [12]	PIV	5000	10	1.2	5.9
Furuichi et al. [15]	LDV	5000	12	1.5	6

JSR A
Journal of Scientific Reports

Aider and Danet [26]	LES	5100	4	1.2	5.8
Kang and Choi [38]	LES	5100	4	1.2	6.2
Present study	k-ε RNG	5000	12	1.5	5.92

The value has been obtained with percentage error of 1.33 % compared to the reference result given by Furuichi et al. [15]. Furthermore, the reattachment length of the present study has been attained by with percentage error of 0.34 % with respect to the value presented by Scarano et al. [12] in terms of same Reynolds number. In case of similar Reynolds number, the numerical result is also close to the values obtained by Aider and Danet [26] and Kang and Choi [38]. With respect to these results, the present result is in good agreement.

3. RESULTS AND DISCUSSION

Flow characteristics over a backward-facing step have been numerically examined via k-ε RNG turbulence model for Re = 5000. Numerical results including pressure distributions, streamwise and cross-stream velocity components, velocity magnitude values with streamline patterns and turbulence kinetic energy values have been given for planes at z* = 0, respectively. Moreover, the contour graphics for streamwise velocity components have been presented for planes in a row at $0 \leq x^* \leq 7$. Pressure values have been shown for eight stations in a row. The stations have been given for x* = 0, 1, 2, 3, 4, 5, 6 and 7, respectively. Same stations have been used for the exhibitions of streamwise velocity components and turbulence kinetic energy values.

Pressure distributions have been presented for $-0.2 \leq P^* = P / (\rho U_\infty^2) \leq 0.0005$ as depicted in Figure 5 at z* = 0. Pressure values indicated decrement owing to effect of backward-facing step flow and the pressure drop was clearly observed for the downstream. Flow separation from the edge of the step has been obtained and pressure values have changed. Lower pressure zone for the wake region has been attained. Rotational flow structure has been seen as anticipated. Gradual pressure distributions have been provided for the channel as stated by Goktepeli et al. [39]. Due to flow recovery, increasing pressure values have been seen. This situation is effective after the flow reattachment point. Since the cross-sectional area of the duct increases, fluid velocity decreases and pressure value reversely increases as expected.

JSR A
Journal of Scientific Reports

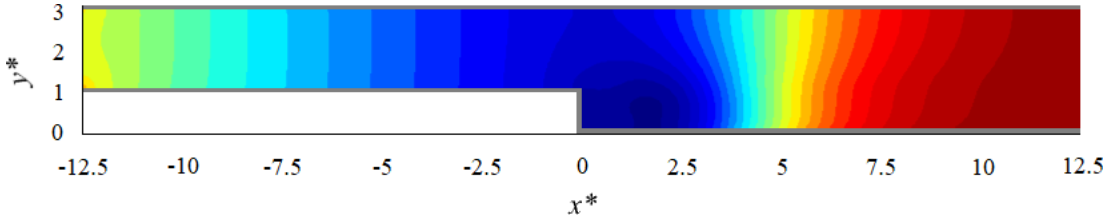

Figure 5. Pressure distributions along the channel.

Streamwise velocity component values of $-0.2 \leq u^* = u / U_\infty \leq 1.08$ have been shown in Figure 6 for $z^* = 0$. The peak value for this component has been attained around the channel axis. However, minimum value has been obtained in the wake region. Before the flow reattachment, negative values have been observed. Rotational flow structures have been observed with the negative velocity values as in the study done by Goktepeli et al. [40]. The upstream boundary layer has indicated separation from the edge and became a curved one as quasi-boundary. A large vorticity has occurred inside the aforementioned zone. Furthermore, a smaller one through the step depth has been spotted.

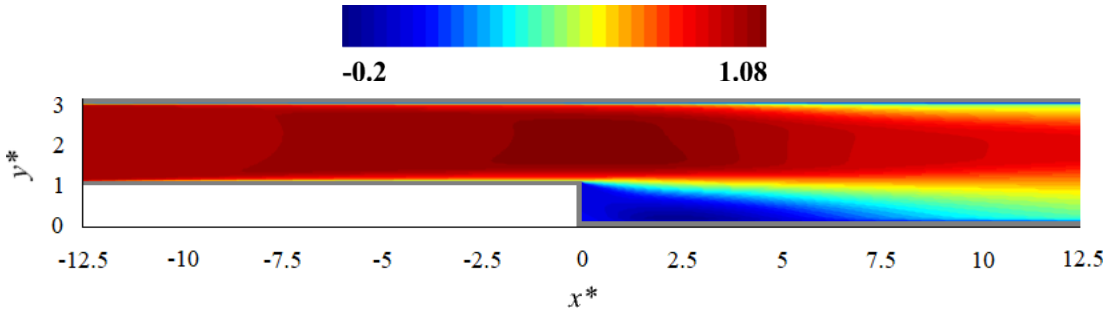

Figure 6. Streamwise velocity components along the channel.

Cross-stream velocity components have been given in Figure 7 for the range of $-0.056 \leq v^* = v / U_\infty \leq 0.056$ as shown. The peak value has been attained in the wake region of the backward-facing step. Flow separation is responsible for this distribution. Nevertheless, minimum value of this component has been observed for $3 \leq x^* \leq 7$ and $0.5 \leq y^* \leq 1.5$. The size of the cluster with negative values is larger than that of the cluster with positive values. Approximately average values have been attained for the rest of the duct.

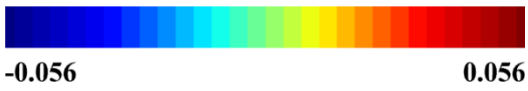

JSR A
Journal of Scientific Reports

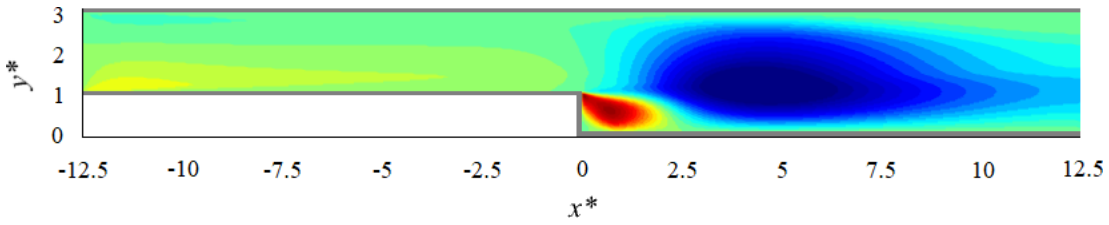

Figure 7. Cross-streamwise velocity components along the channel.

Velocity magnitude values with streamline patterns have been presented for the plane at z* = 0 as in Figure 8. The vorticity for the wake in terms of x* < 5.92 has been seen. This vorticity has occurred because of separated flow. As expected, flow separation triggers a lower pressure region [41, 42]. A small vorticity has been observed in the wake region close to the bottom edge. It is called as a secondary eddy.

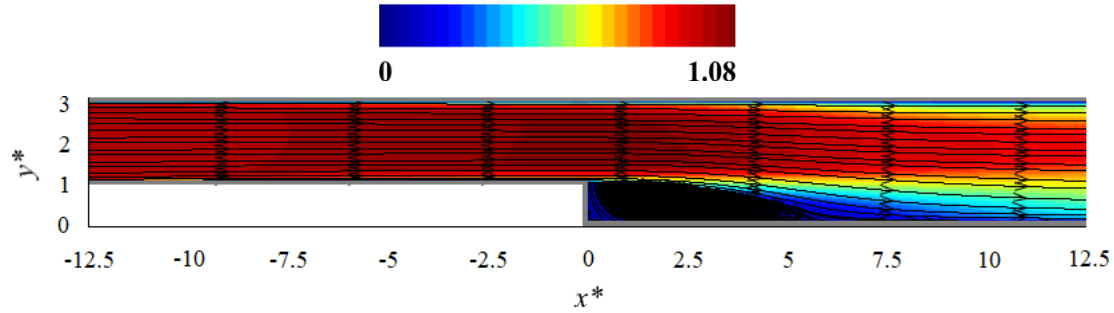

Figure 8. Velocity magnitude values with streamline patterns along the channel.

Turbulence kinetic energy values have been exhibited for $0.0016 \leq TKE^* = TKE / U_\infty^2 \leq 0.048$ in Figure 9. Kinetic energy is defined for the mean flow conditions. When attaining kinetic energy of the turbulent flow structure, turbulence kinetic energy (TKE) is utilized as a term, and it depends on turbulence density of the flow field [39]. Minimum value has been affected via core flow around the duct axis. However, it is not clearly valid for maximum value. With influence of turbulence triggered by flow separation, the highest value has been obtained in the wake region. It is a deduction that turbulence level of the step wake is higher than those of any other points.

JSR A
Journal of Scientific Reports

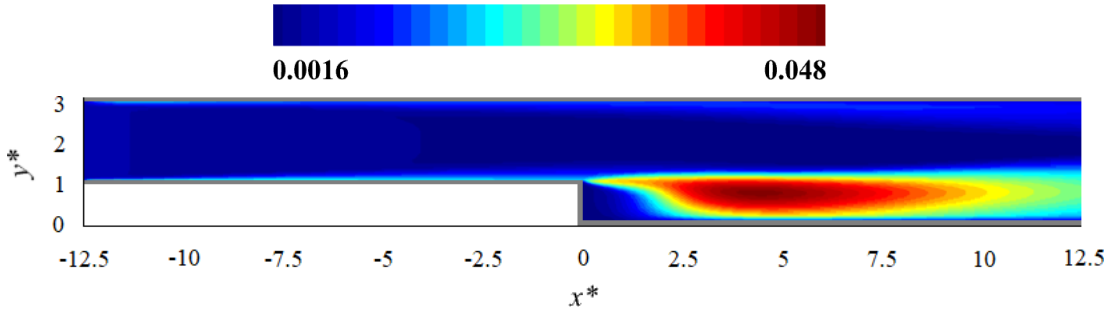

Figure 9. Turbulence kinetic energy values along the channel.

Streamwise velocity components of $-0.2 \leq u^* = u / U_\infty \leq 1.08$ have also been indicated on the planes in a row for x* = 0, 1, 2, 3, 4, 5, 6 and 7 as in Figure 10. Maximum value has been attained around the channel axis. However, minimum value for this component has been attained in the wake region of the step. Negative values have been observed before the flow reattachment point at x* = 5.92 as seen. Rotational flows were effective as stated previously. The upstream boundary layer has separated from the surface and formed as a curved one via quasi-boundary. A large vorticity has occurred and a smaller one through the step depth has also been detected. Moreover, symmetrical flow patterns have been spotted with respect to the line crossing through z* = 0.

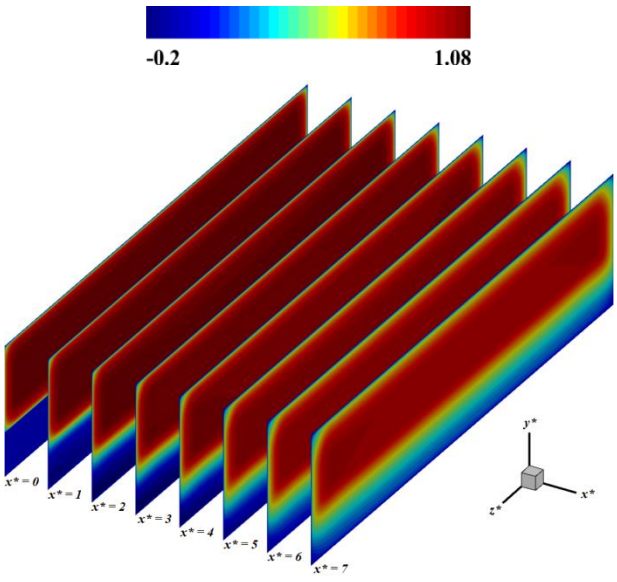

Figure 10. Streamwise velocity components on various stations.

JSR A
Journal of Scientific Reports

Pressure distributions along the x-axis have been given for y* = 1 and y* = 2 at z* = 0 as in Figure 11. For the upstream region of the backward-facing step, pressure drop has been obtained. The reason is that cross-sectional area is narrower. Depending on this case, velocity value for fluid flow is higher. However, pressure tends to increase for the downstream zone of the backward-facing step. Because there is an expansion for the cross-section. For this reason, velocity value is getting lower. On the other hand, pressure values have been increased. When the pressure difference between y* = 1 and y* = 2 is investigated, pressure values of y* = 1 are lower than those of y* = 2 for the first part of the downstream. However, it is vice versa for the second part of the downstream. This trend has been affected by interaction between flow separation and wake flow.

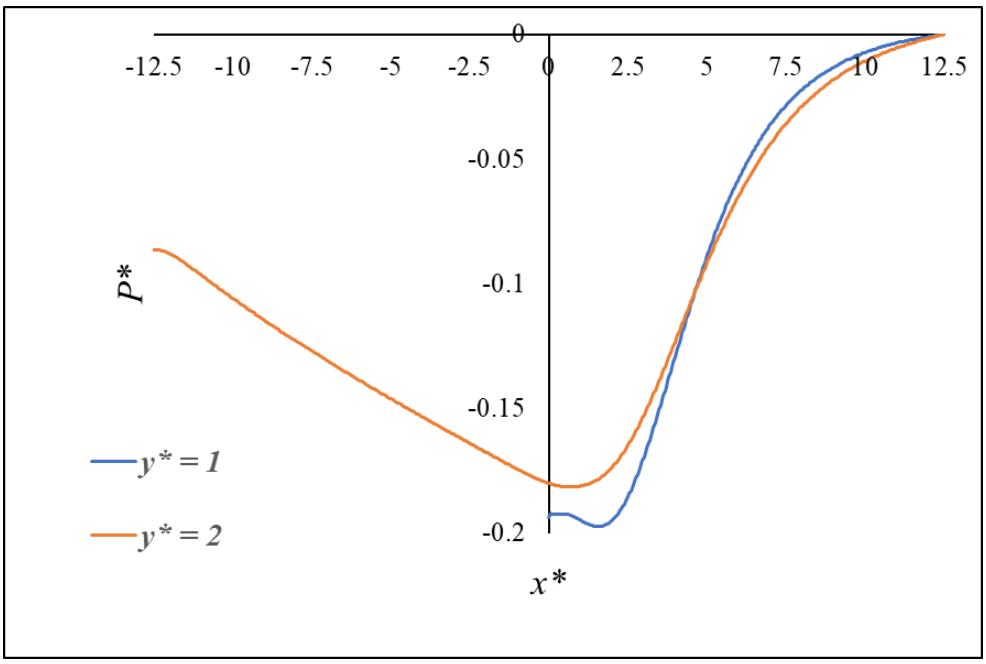

Figure 11. Pressure distributions for different stations.

Velocity profiles of streamwise components have been presented for $0 \leq x^* \leq 7$ at z* = 0 as in Figure 12. Evolution of velocity profiles has been observed in a row in terms of the region covering flow separation and its reattachment inside the step wake. For the investigated part of the duct, streamwise velocity components are in the range of $-0.2 \leq u^* \leq 1.1$ as seen. Rotational flows are indicated by negative values which are dominant for $1 \leq x^* \leq 5$ in the chart. Since there is not any element disrupting the flow at the upstream, all values are positive as expected. Same situation has also been detected for x* > 6 as flow reattachment is completed. In addition to the first reason, the effect of the wake region has also disappeared. Transition to core flow has been obtained at y* = 1.1 which is above the step height. In that point, same velocity value of u* = 0.75 has been provided.

JSR A
Journal of Scientific Reports

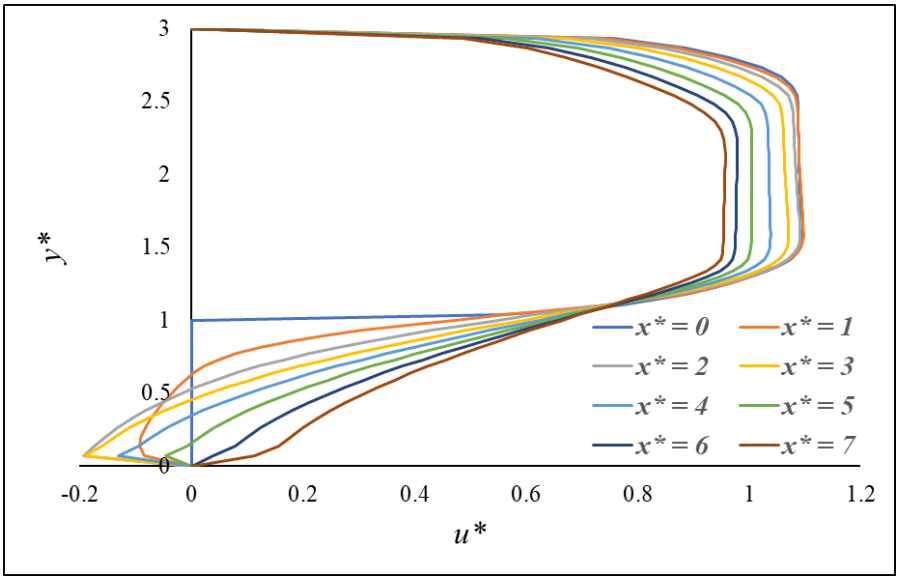

Figure 12. Velocity profiles of streamwise components for different stations.

Turbulence kinetic energy values have also been given for $0 \leq x^* \leq 7$ at $z^* = 0$ as in Figure 13. As explained previously, kinetic energy is valid in case of average flow conditions. When obtaining kinetic energy of the turbulent flow field, turbulence kinetic energy (TKE) is the required terms based on turbulence density of the flow structure. Change of these values has been presented in a row and the zone for separated and reattached flow in the wake region has been defined. Turbulence kinetic energy values have been given for $0 \leq TKE^* \leq 0.05$ for the related section of the channel. Flow oscillations have been observed for $x^* \geq 2$ and $y^* \leq 1$ since the fluctuations for these values are effective in the wake region.

JSR A
Journal of Scientific Reports

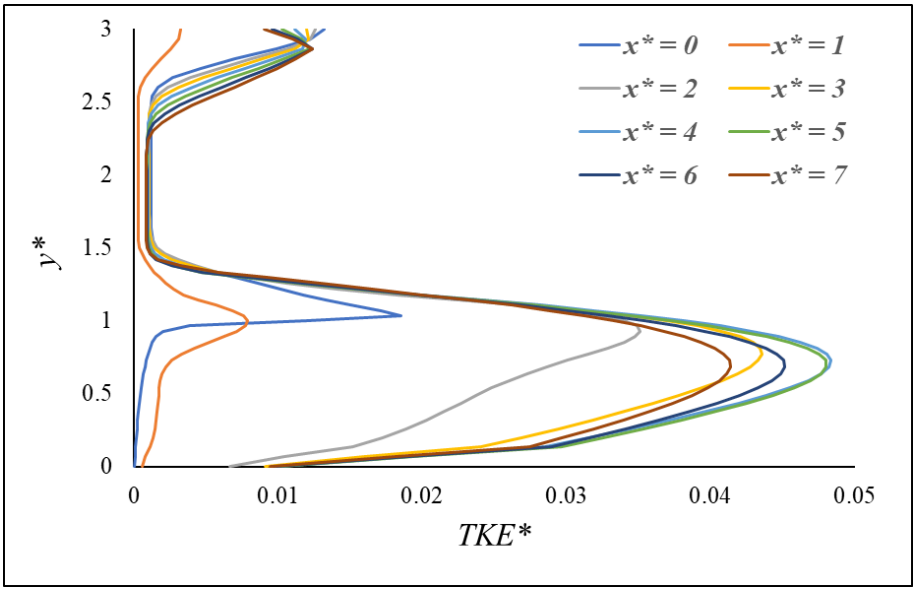

Figure 13. Turbulence kinetic energy values for different stations.

There is difference between the values from neighbor points. It is the indicator that turbulence intensity is higher at any related points. As there is not any element disrupting the core flow, the fluctuations in these values are limited.

4. CONCLUSIONS

In the present study, backward-facing step flow has been modeled with respect to an experimental study done at Re = 5000. Steady simulations have been conducted regarding the same flow conditions of the reference study. Pressure distributions, streamwise and cross-stream velocity components, velocity magnitude values with streamline patterns and turbulence kinetic energy values have been presented by using contour graphics. Furthermore, the stations for pressure distributions, velocity profiles for streamwise components and turbulence kinetic energy values have been defined for evolution of related data. The obtained results could be outlined as followings:

- The turbulence models of Standard k-ε, k-ε RNG, k-ε Realizable, Standard k-ω and k-ω SST have been tested. In terms of reattachment length, k-ε RNG turbulence model has been chosen and numerical solutions have been done.
- Lower pressure zone for the wake region of the backward-facing step has been attained due to flow separation.
- Separation of the upstream boundary layer has been seen and it became a curved one.
- What is more, turbulence level of the step wake has been obtained as higher than those of any other points.

- Transition to core flow has been attained at $y^* = 1.1$ that is above the step height.
- Flow oscillations have been observed for $x^* \geq 2$ and $y^* \leq 1$ since the fluctuations for these values are effective in the wake region.
- The dimensionless reattachment length has been numerically obtained as 5.92 which is very good agreement with the experimental results at same Reynolds number. The deviation from the reference results is from 0.34 % to 1.33 % in terms of percentage errors.

Since the backward-facing step flow including flow separation and its reattachment, it is very significant for engineering applications as airfoils, buildings, heat exchangers, hydrofoils, spoilers, turbine blades, combustor flame-holder and engine inlets, micro combustors. Flow behavior is influenced owing the change of channel height for flow direction. For this reason, the expansion effect should be considered and investigated via experimental and numerical methods. Considering the non-availability of experimental facilities, numerical modeling with reliable methods is very important. Use and comparison of other turbulence models is recommended for future studies on the backward-facing step flow.

ACKNOWLEDGMENT

The present study has been supported by Konya Technical University Academic Staff Training Program with the project number of 2018-OYP-046.

REFERENCES

[1] Chen, L., Asai, K., Nonomura, T., Xi, G. and Liu, T., (2018). A review of backward-facing step (BFS) flow mechanisms, heat transfer and control, Thermal Science and Engineering Progress, 6, 194-216.

[2] Teso-Fz-Betoño, D., Juica, M., Portal-Porras, K., Fernandez-Gamiz, U. and Zulueta, E., (2021). Estimating the reattachment length by realizing a comparison between URANS k-omega SST and LES WALE models on a symmetric geometry, Symmetry, 13(9), 1555.

[3] Arthur, J.K., (2023). A narrow-channeled backward-facing step flow with or without a pin–fin insert: Flow in the separated region, Experimental Thermal and Fluid Science, 141, 110791.

[4] Detto, M., Katul, G.G., Siqueira, M., Juang, J.Y. and Stoy, P., (2008). The structure of turbulence near a tall forest edge: The backward-facing step flow analogy revisited, Ecological Applications, 18(6), 1420-1435.

[5] Deepa, G. and Murali, G., (2014). Effects of viscous dissipation on unsteady MHD free convective flow with thermophoresis past a radiate inclined permeable plate, Iranian Journal of Science and Technology, 38(3.1), 379-388.

[6] Jiaqiang, E., Cai, L., Li, J., Ding, J., Chen, J. and Luo, B., (2022). Effects analysis on the catalytic combustion and heat transfer performance enhancement of a non-premixed hydrogen/air micro combustor, Fuel, 309, 122125.

[7] Zuo, W., Zhao, H., Jiaqiang, E., Li, Q. and Li, D., (2022). Numerical investigations on thermal performance and flame stability of hydrogen-fueled micro tube combustor with injector for thermophotovoltaic applications, International Journal of Hydrogen Energy, 47(39), 17454-17467.

[8] Giannopoulos, A. and Aider, J.L., (2020). Prediction of the dynamics of a backward-facing step flow using focused time-delay neural networks and particle image velocimetry data-sets, International Journal of Heat and Fluid Flow, 82, 108533.

[9] Oder, J., Shams, A., Cizelj, L. and Tiselj, I., (2019). Direct numerical simulation of low-Prandtl fluid flow over a confined backward facing step, International Journal of Heat and Mass Transfer, 142, 118436.

[10] Jovic, S. and Driver, D., (1995). Reynolds number effect on the skin friction in separated flows behind a backward-facing step, Experiments in Fluids, 18, 464-467.

[11] Kasagi, N. and Matsunaga, A., (1995). Three-dimensional particle-tracking velocimetry measurement of turbulence statistics and energy budget in a backward-facing step flow, International Journal of Heat and Fluid Flow, 16(6), 477-485.

[12] Scarano, F., Benocci, C. and Riethmuller, M.L., (1999). Pattern recognition analysis of the turbulent flow past a backward facing step, Physics of Fluids, 11(12), 3808-3818.

[13] Wengle, H., Huppertz, A., Bärwolff, G. and Janke, G., (2001). The manipulated transitional backward-facing step flow: an experimental and direct numerical simulation investigation, European Journal of Mechanics-B/Fluids, 20(1), 25-46.

[14] Kostas, J., Soria, J. and Chong, M., (2002). Particle image velocimetry measurements of a backward-facing step flow, Experiments in Fluids, 33, 838-853.

[15] Furuichi, N., Hachiga, T. and Kumada, M., (2004). An experimental investigation of a large-scale structure of a two-dimensional backward-facing step by using advanced multi-point LDV, Experiments in Fluids, 36, 274-281.

[16] Nie, J.H. and Armaly, B.F., (2004). Reverse flow regions in three-dimensional backward-facing step flow, International Journal of Heat and Mass Transfer, 47(22), 4713-4720.

[17] Schram, C., Rambaud, P. and Riethmuller, M.L., (2004). Wavelet based eddy structure eduction from a backward facing step flow investigated using particle image velocimetry, Experiments in Fluids, 36, 233-245.

[18] Bouda, N.N., Schiestel, R., Amielh, M., Rey, C. and Benabid, T., (2008). Experimental approach and numerical prediction of a turbulent wall jet over a backward facing step, International Journal of Heat and Fluid Flow, 29(4), 927-944.

[19] Wu, Y., Ren, H. and Tang, H., (2013). Turbulent flow over a rough backward-facing step, International Journal of Heat and Fluid Flow, 44, 155-169.

[20] Nadge, P.M. and Govardhan, R.N., (2014). High Reynolds number flow over a backward-facing step: structure of the mean separation bubble, Experiments in Fluids, 55, 1-22.

[21] Yamada, S. and Nakamura, H., (2016). Construction of 2D-3C PIV and high-speed infrared thermography combined system for simultaneous measurement of flow and thermal fluctuations over a backward facing step, International Journal of Heat and Fluid Flow, 61, 174-182.

[22] Le, H., Moin, P. and Kim, J., (1997). Direct numerical simulation of turbulent flow over a backward-facing step, Journal of Fluid Mechanics, 330, 349-374.

[23] Chiang, T.P., Sheu, T.W. and Fang, C.C., (1999). Numerical investigation of vortical evolution in a backward-facing step expansion flow, Applied Mathematical Modelling, 23(12), 915-932.

[24] Avancha, R.V. and Pletcher, R.H., (2002). Large eddy simulation of the turbulent flow past a backward-facing step with heat transfer and property variations, International Journal of Heat and Fluid Flow, 23(5), 601-614.

[25] Dejoan, A. and Leschziner, M.A., (2004). Large eddy simulation of periodically perturbed separated flow over a backward-facing step, International Journal of Heat and Fluid Flow, 25(4), 581-592.

[26] Aider, J.L. and Danet, A., (2006). Large-eddy simulation study of upstream boundary conditions influence upon a backward-facing step flow, Comptes Rendus Mécanique, 334(7), 447-453.

[27] Barri, M., El Khoury, G.K., Andersson, H.I. and Pettersen, B., (2010). DNS of backward-facing step flow with fully turbulent inflow, International Journal for Numerical Methods in Fluids, 64(7), 777-792.

[28] El Khoury, G.K., Andersson, H.I., Barri, M. and Pettersen, B., (2010). Massive separation of turbulent Couette flow in a one-sided expansion channel, International Journal of Heat and Fluid Flow, 31(3), 274-283.

[29] Jürgens, W. and Kaltenbach, H.J., (2012). The effect of sweep on the forced transitional flow over a backward-facing step, Computers and Fluids, 59, 1-10.

[30] Kanchi, H., Sengupta, K. and Mashayek, F., (2013). Effect of turbulent inflow boundary condition in LES of flow over a backward-facing step using spectral element method, International Journal of Heat and Mass Transfer, 62, 782-793.

[31] Togun, H., Safaei, M.R., Sadri, R., Kazi, S.N., Badarudin, A., Hooman, K. and Sadeghinezhad, E., (2014). Numerical simulation of laminar to turbulent nanofluid flow and heat transfer over a backward-facing step, Applied Mathematics and Computation, 239, 153-170.

[32] Amiri, A., Arzani, H.K., Kazi, S.N., Chew, B.T. and Badarudin, A., (2016). Backward-facing step heat transfer of the turbulent regime for functionalized graphene nanoplatelets based water–ethylene glycol nanofluids, International Journal of Heat and Mass Transfer, 97, 538-546.

[33] Xu, J.H., Zou, S., Inaoka, K. and Xi, G.N., (2017). Effect of Reynolds number on flow and heat transfer in incompressible forced convection over a 3D backward-facing step, International Journal of Refrigeration, 79, 164-175.

[34] Yagmur, S., Dogan, S., Aksoy, M.H. and Goktepeli, I., (2020). Turbulence modeling approaches on unsteady flow structures around a semi-circular cylinder, Ocean Engineering, 200, 107051.

[35] Goktepeli, I. and Atmaca, U., (2023). Examination of air flow characteristics over an open rectangular cavity between the plates, International Journal of Aeroacoustics, 22(3-4), 351-370.

[36] Murali, G., Paul, A.J.I.T. and Narendrababu, N.V., (2015). Numerical study of chemical reaction effects on unsteady MHD fluid flow past an infinite vertical plate embedded in a porous medium with variable suction, Electronic Journal of Mathematical Analysis and Applications, 3(2), 179-192.

[37] Murali, G. and Narendrababu, N.V., (2021). Convective MHD jeffrey fluid flow due to vertical plates with pulsed fluid suction: A numerical study, Journal of Computational Applied Mechanics, 54(1), 36-48.

[38] Kang, S. and Choi, H., (2002). Suboptimal feedback control of turbulent flow over a backward-facing step, Journal of Fluid Mechanics, 463, 201-227.

[39] Goktepeli, I., Atmaca, U. and Cakan, A., (2020). Investigation of heat transfer augmentation between the ribbed plates via Taguchi approach and computational fluid dynamics, Journal of Thermal Science, 29, 647-666.

[40] Goktepeli, I., Atmaca, U. and Yagmur, S., (2021). Visualization of flow characteristics between the ribbed plates via Particle Image Velocimetry, Thermal Science, 25(1), 171-179.

[41] Goktepeli, I. and Atmaca, U., (2020). Numerical examination of heat transfer augmentation between the plates with square cross-sectional ribs for the staggered arrangement, Kocaeli Journal of Science and Engineering, 3(2), 33-40.

[42] Goktepeli, I. and Atmaca, U., (2021). Computational study on the effect of the staggered ribs on heat transfer phenomena between the horizontal plates, Hittite Journal of Science and Engineering, 8(1), 7-17.